crystals

MDPI

Article

Site Selectivity of Halogen Oxygen Bonding in 5- and 6-Haloderivatives of Uracil

Gustavo Portalone

Department of Chemistry, 'Sapienza' University of Rome, 00185 Rome, Italy; gustavo.portalone@uniroma1.it; Tel.: +396-4991-3715

Received: 5 August 2019; Accepted: 25 August 2019; Published: 6 September 2019

Abstract: Seven 5-and 6-halogenated derivatives of uracil or 1-methyluracil (halogen = Cl, Br, I) were studied by single crystal X-ray diffraction. In contrast with pure 5-halouracils, where the presence of N-H···O and C-H···O hydrogen bonds prevents the formation of other intermolecular interactions, the general ability of pyrimidine nucleobases to provide electron donating groups to halogen bonding was confirmed in three crystals and cocrystals containing uracil with the halogen atom at the C6 position. In the latter compounds, among the two nucleophilic oxygen atoms in the C=O moiety, only the urea carbonyl oxygen O1 can act as halogen bond acceptor, being not saturated by conventional hydrogen bonds. The halogen bonds in pure 6-halouracils are all rather weak, as supported by Hirshfeld surface analysis. The strongest interaction was found in the structure of 6-iodouracil, which displayed the largest (13%) reduction of the sum of van der Waals (vdW) radii for the contact atoms. Despite this, halogen bonding plays a role in determining the crystal packing of 6-halouracils, acting alongside conventional hydrogen bonds.

Keywords: halouracils; halonucleobases; halogen bond

1. Introduction

Over the past two decades, it has been well recognized that the diversity of non-covalent interactions involving halogen compounds are topical in biology, materials science, and crystal engineering [1,2]. Although hydrogen bonding (HB) is commonly the predominant interaction, the biological significance of halogen bonding (XB) has been widely demonstrated [3].

XB is a stabilizing directional interaction due to an attraction between the positively charged area of a covalently bound halogen atom and an electron donor species. As the halogen polarizability is the key factor in XB, the strength of the halogen bonding is expected to decrease in the order I > Br > Cl ≫ F [4]. Several examples of XB have been culled from a comprehensive survey of halogenated protein and nucleic acid structures in the Protein Data Bank. Interestingly, it has been shown that an unusually strong Br···O intermolecular contact, 2.7 Å, i.e., 0.8 times the sum of van der Waals (vdW) radii for Br and O atoms, involving 5-bromouracil stabilizes a Holliday junction [5]. In this context, 5- and 6-halogenated derivatives of uracil have raised special attention as coformers of cocrystals of active pharmaceutical ingredients, due to their capability to form supramolecular assemblies through XBs and HBs [6].

Despite the potential of 5- and 6-haloderivatives of uracil for crystal engineering (5Xuras and 6Xuras, respectively, X = Cl, Br, and I), a search of crystal structures containing 5Xura or 6Xura units (excluding metallic elements) with the Cambridge Structural Database (CSD, version 5.40 updated to May 2019) [7], surprisingly yielded only 38 unique hits with 5Xura, and only three unique hits with 6Xura (CSD refcodes: QECNOB, ZUDTAV and ZUDTAV01). Adopting a cutoff value of 0.92 for the interaction ratio R_{XB} [8], the ratio between the X···A (A = acceptor) contacts showing linear C-X···A disposition (bond angle > 155°) and the sum of vdW radii, 16 out of the 38 structures for 5Xuras and

two out of the three structures for 6Xuras manifest weak linear XB interaction in which halogen atoms function as a XB donor. Out of the 18 structures showing XBs, 5-iodouracil and 6-chlorouracil can act as a XB donor only when cocrystallized with polar solvents [9,10] or with aminoazine derivatives [11]. Only eight structures containing the 5Xura fragment show XB interactions with nucleobases, with no clear evidence for the preferred nucleophilic oxygen, as in four structures O1 and in four structures O2 act as XB acceptors.

Interestingly, in pure 5-halouracils the formation of conventional N-H···O hydrogen bonds is favored over XB interactions. No information concerning the crystal structure of pure 6-halouracils has been found in literature. In *N*,*N*-dimethyl-5-bromo-, *N*,*N*-dimethyl-5-iodouracil and their (1:1) cocrystal, where the *N*-methylation at the 1 and 3 positions prevents the formation of strong HB, halogen and unconventional (C-H···O) hydrogen bonds play an equally important role in the overall crystal structure [8].

In a continuation of a long-term interest in crystal engineering of DNA/RNA bases [12–21] and in systems exhibiting halogen bonding via alternative donors [8,11], this work focuses on the XBs exhibited by pyrimidine nucleobases carrying at the C6 position a halogen atom and at the C2 and the C4 positions two nucleophilic oxygen atoms. This investigation was then extended to the two new polymorphs obtained for 5-chloro and 5-bromouracil and their (1:1) cocrystal (Scheme 1). Thus, the chosen systems should offer the possibility of studying in pure compounds, and their mixed cocrystals, the existence and the preferred donor and acceptor sites for halogen bond formation in the presence of competing conventional and unconventional HBs.

1-methyl-5-bromouracil (5Br1Mura, 4) was determined more than 40 years ago [22], (CSD refcode: MBURAC). In this study, intensity data were collected at room temperature on an equi-inclination Weissenberg camera using Cu Kα radiation. A total of 935 visually estimated reflexions were used in the final least-squares refinement (R = 0.12 for 111 refined parameters). No coordinates are available from CSD for this structure. Consequently, as 5Br1Mura can be considered as simple model of halouridine, in which deoxyribose attaches to uracil at the N1 atom, a new determination of the crystal structure of 5Br1Mura was warranted to improve the precision of the geometric parameters and to investigate the occurrence of halogen bonds.

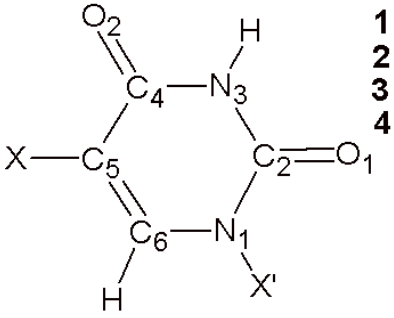

1 X,X' = Cl, H 5Clura
2 Br, H 5Brura
3 Cl/Br, H 5Cl5Brura
4 Br, CH_3 5Br1Mura

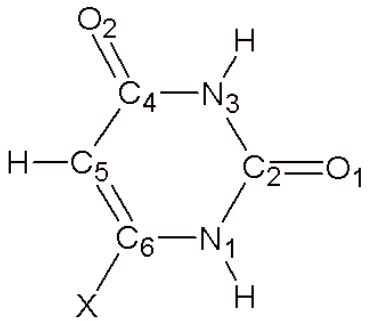

5 X = Cl 6Clura
6 I 6Iura
7 Cl/CH_3 6Cl6Mura

Scheme I. Chemical structures of compounds investigated in this study and the adopted atom-numbering scheme.

Interestingly, the subtle competition between hydrogen and halogen bonding, as they often manifest comparable energies, has been recently studied by applying a protocol based on DFT calculations at high level of theory and topological analysis of the electron density distribution within the formalism of Bader's theory (Quantum Theory of Atoms in Molecules, QTAIM method) [23]. This theoretical approach provided an accurate estimate of the energies of supramolecular contacts involved in the halogen bonding-assisted crystal packing of metal halide complexes with halopyridinium cations [24,25].

2. Materials and Methods

2.1. Crystal Preparation

The 5- and 6-halouracils were purchased from Aldrich with 95%–99% purity and were subjected to further purification by successive sublimation under reduced pressure. The solvents employed for the crystallization were of reagent grade. In the case of pure compounds, 0.1 mmol was taken in an agate mortar and pestle, and then a few drops of liquid (*N,N*-dimethylformamide, DMF) were added. In the case of cocrystals, equimolecular amounts (1:1, 0.1mmol) were taken in an agate mortar and pestle, and then liquid (DMF) assisted co-grinding was performed on each mixture. Crystallization of ground powders were adjusted in a set of different solvents (or mixture of solvents). The resulting solutions (1−2 mL) were heated at 70 °C, stirred for 12 h under reflux, and then cooled to room temperature and filtered. Good quality crystals were obtained from slow room-temperature evaporation of DMF solutions after 1−2 weeks.

2.2. Single Crystal Structure Analysis

The crystallographic data and details of data collection and structure refinement are summarized in Table 1. Diffraction data were obtained on an Oxford Diffraction Xcalibur S CCD diffractometer (Oxford Diffraction, Oxford, England) (graphite-monochromated Mo Kα radiation, λ = 0.710689 Å) at room temperature. Integration and absorption corrections were performed using the CrysAlisPro software package (Agilent Technologies Ltd: Yarnton, Oxfordshire, England) [26]. The crystal structures were solved by direct methods using SIR2004 [27], and refined by the full-matrix least-squares method based on F^2 using SHELXL-2014/7 [28], within the WinGX system [29]. For all structures, nonhydrogen atoms were refined anisotropically. The hydrogen atoms were located by Fourier synthesis and refined freely. Positions of carbon-bound H atoms were calculated geometrically [C−H = 0.97 Å, Uiso (H) values equal to 1.2 Ueq(C) for aromatic or 1.5 Ueq(C) for methyl H atoms] and refined in the riding model. Free rotation about the local three-fold axis was then allowed for all methyl groups. The molecular and packing diagrams were prepared with the Mercury 3.9 program package [30]. The isomorphic 5-chlorouracil (5Clura) 5-bromouracil (5Brura) and 5-chloro uracil/5bromouracil (5Cl5Brura) structures exhibit different disorder. In the 5Clura and 5Brura structures, each molecule in the asymmetric unit is disordered between two orientations generated by a mirror perpendicular to the molecular plane. This disorder was modeled over two sites, assigning equal values (0.5) to the site occupancy factor of each component in the two orientations. The (1:1) 5-chlorouracil/5-bromouracil structure, along with the orientational disorder, shows Cl(1) and Br(1) disorder. This disorder was treated assigning equal values (0.25) to site occupancy factors of both atoms. The (1:1) 6-chlorouracil/6-methyluracil structure, 6Cl6Mura, shows Cl(1) and C(7) disorder. This disorder was modeled over two sites, with the aid of constraints on occupancy factors, and the ratio between Cl(1)/C(7) occupied sites was about 0.6:0.4. Several trials of data collection at LT using crystals mounted under paraffin oil in a nylon loop failed, as the samples cracked when slowly cooled in liquid nitrogen. CCDC 1943002–1943008 contains the supplementary crystallographic data for this paper. These data can be obtained free of charge via http://www.ccdc.cam.ac.uk/conts/retrieving.html (or from the CCDC, 12 Union Road, Cambridge CB2 1EZ, UK; Fax: +44 1223 336033; E-mail: deposit@ccdc.cam.ac.uk). The Hirshfeld surface analysis was carried out using Crystal Explorer 3.1 (University of Western Australia: Crawley, AU, Australia) [31] with final refined crystallographic information files as input. Ortep diagrams for the seven compounds reported in the paper can be found in the Electronic Supplementary Information (see Figures S1 to S7).

Table 1. Crystal data, data collection, and refinement for compounds 1–7.

Crystal	1, 5Clura	2, 5Brura	3, 5Cl5Brura	4, 5Br1Mura
Crystal data				
Chemical formula	$C_4H_3ClN_2O_2$	$C_4H_3BrN_2O_2$	$C_8H_6BrClN_4O_4$	$C_5H_5BrN_2O_2$
M_r	146.53	191.0	337.52	205.02
Crystal system	Monoclinic	Monoclinic	Monoclinic	Monoclinic
Space group	$P2_1/m$	$P2_1/m$	$P2_1/m$	$P2_1/c$
a (Å)	5.5150 (12)	5.7154 (8)	5.6270 (6)	7.1787 (11)
b (Å)	6.8639 (18)	6.8825 (12)	6.8631 (9)	12.3056 (10)
c (Å)	7.126 (2)	7.1928 (11)	7.1582 (9)	7.7021 (12)
β (°)	96.92 (2)	97.380 (14)	97.292 (11)	91.275 (15)
V (Å^3)	267.78 (12)	280.60 (8)	274.20 (6)	680.22 (16)
Z	2	2	1	4
μ(mm^{-1})	0.62	7.24	4.01	5.98
Crystal size (mm)	0.12 × 0.11 × 0.08	0.11 × 0.09 × 0.08	0.12 × 0.09 × 0.08	0.15 × 0.12 × 0.10
Data collection				
T_{min}, T_{max}	0.816, 1.000	0.465, 1.000	0.351, 1.000	0.227, 1.000
No. of measured, independent, observed [$I > 2\sigma(I)$] reflections	5270 844 694	5619 959 797	5922 937 800	13317 1978 1510
R_{int}	0.037	0.039	0.077	0.044
(sin $\theta/\lambda)_{max}$ (Å^{-1})	0.704	0.725	0.725	0.703
Refinement				
$R[F^2 > 2\sigma(F^2)]$	0.035	0.029	0.032	0.039
$wR(F^2)$	0.095	0.072	0.081	0.095
S	1.05	1.09	1.10	1.06
No. of parameters	55	59	65	96
$\Delta\rho_{max}$, $\Delta\rho_{min}$ (e Å^{-3})	0.34, −0.22	0.47, −0.67	0.37, −0.31	0.52, −0.56

Crystal	5, 6Clura	6, 6Iura	7, 6Cl6Mura
Crystal data			
Chemical formula	$C_4H_3ClN_2O_2$	$C_4H_3IN_2O_2$	$C_{4.42}H_{4.26}Cl_{0.58}N_2O_2$
M_r	146.53	237.98	137.91
Crystal system	Monoclinic	Monoclinic	Monoclinic
Space group	$P2_1/c$	$P2_1/c$	$P2_1/c$
a (Å)	4.7850 (8)	5.0339 (5)	4.7297 (8)
b (Å)	10.2750 (12)	10.920 (1)	10.4449 (17)
c (Å)	11.6185 (13)	11.6673 (13)	11.6798 (18)
β (°)	96.858 (12)	99.034 (10)	97.612 (14)
V (Å^3)	567.15 (13)	633.40 (11)	571.91 (16)
Z	4	4	4
μ (mm^{-1})	0.59	4.98	0.38
Crystal size (mm)	0.12 × 0.09 × 0.07	0.10 × 0.08 × 0.07	0.11 × 0.09 × 0.07
Data collection			
T_{min}, T_{max}	0.533, 1.000	0.595, 1.000	0.605, 1.000
No. of measured, independent,	11,349 1725 966	12,467 1936 1585	8017 1302 1025

observed [$I > 2\sigma(I)$] reflections			
R_{int}	0.105	0.046	0.046
$(\sin\theta/\lambda)_{max}$ (Å^{-1})	0.714	0.714	0.650
Refinement			
$R[F^2 > 2\sigma(F^2)]$	0.055	0.028	0.047
$wR(F^2)$	0.154	0.061	0.115
S	1.05	1.09	1.10
No. of parameters	90	84	101
$\Delta\rho_{max}$, $\Delta\rho_{min}$ (e Å^{-3})	0.26, −0.35	0.56, −0.49	0.17, −0.17

3. Results and Discussion

3.1. Structural Analysis of 5-Halouracils (1–4)

Previous crystallographic studies have shown that 5Clura and 5Brura, 1 and 2 respectively, have two polymorphic forms: the isostructural $P2_1/c$ monoclinic, CLURAC10 and BRURAC10 [32], and the isostructural $P2_1/n$ monoclinic, CLURAC11 and BRURAC11 [33].

In this work, 5Clura and 5Brura both crystallize in a third polymorphic form, $P2_1/m$ monoclinic. Each asymmetric unit contains a single molecule as diketo tautomer laying on a mirror perpendicular to the molecular plane and passing through the O1 C2 C5 X atoms (X = Cl or Br), i.e., there is an interchange of the oxygen and hydrogen atoms on C4 and C6. These two monoclinic forms are isostructural (Figure 1a,b respectively). Consequently, the following discussion of the hydrogen bonding scheme of 5Clura and 5Brura will be the same.

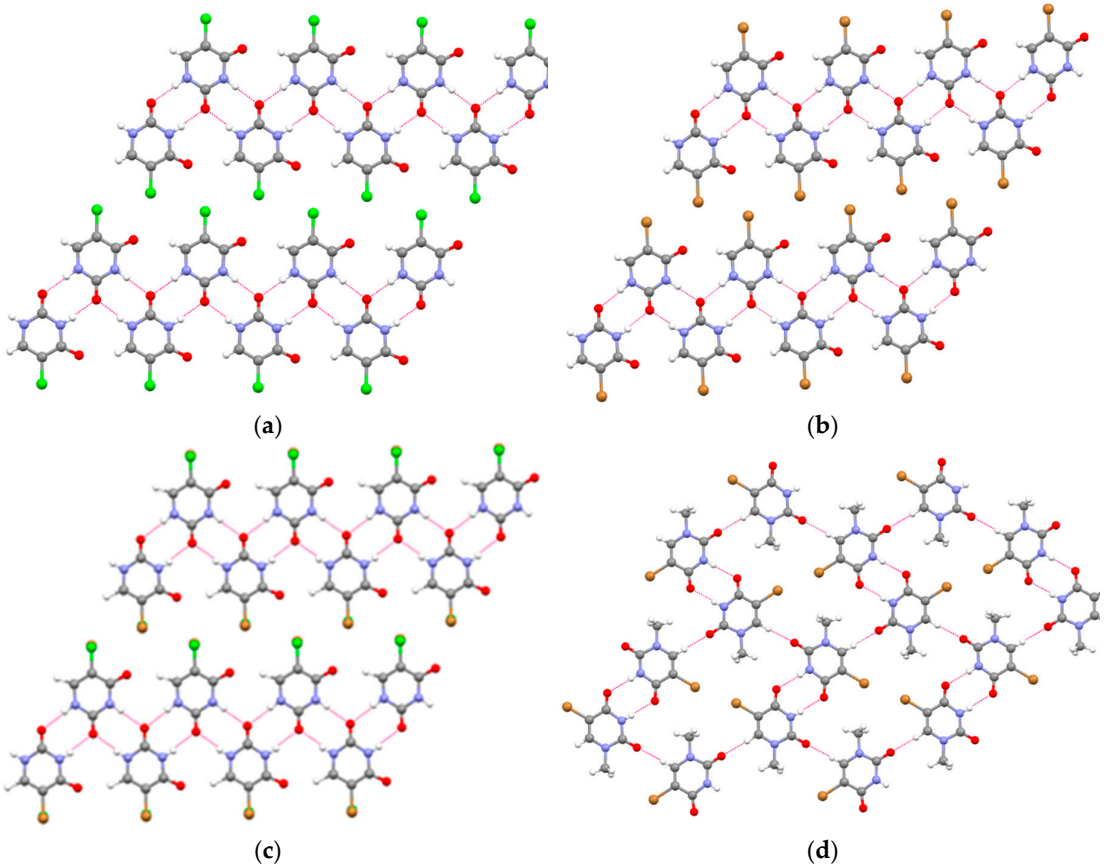

(**a**) (**b**) (**c**) (**d**)

Figure 1. Hydrogen bonding in the crystal packing of 5-halouracils. (**a**) 5Clura. (**b**) 5Brura. (**c**) 5Cl5Brura. (**d**) 5Br1Mura. For the sake of clarity, in (a) and (b) only one of the two sites of the disordered 5Clura and 5Brura molecules is shown. Hydrogen bonds are shown as red dotted lines.

The crystal structures of the $P2_1/m$ monoclinic forms of 5Clura and 5Brura are very similar to those found in the previous monoclinic forms and in thymine monohydrate [12], which can be rationalized with the comparable vdW radii for a methyl group (2.0 Å), bromine (1.85 Å) and, to lesser extent, chlorine (1.81 Å). Parallel symmetric ribbons of planar diketo tautomers associate through N-H···O centrosymmetric hydrogen bonds involving the less hindered O1 oxygen atom (Table 2). These ribbons have been termed as polar, i.e., with all the carbonyl C4=O2 oriented in the same direction within a ribbon [32]. No shorter interatomic contacts have been found for the second carbonyl oxygen O2, other than 3.358 (3) and 3.386 (3) Å, respectively, which occur with the carbon atom C6 of adjacent noncentrosymmetric molecules. The structures also show short C5-Cl(Br)···O2 intermolecular contacts between parallel ribbons [3.265 (2) and 3.412 (2) Å, respectively] that coincide with the cutoff values for XBs (3.27 and 3.37 Å, respectively). No appreciable intermolecular N-H···Cl(Br) HBs are present in the structures.

The crystallographic investigation of the 5Cl5Brura cocrystal, 3, showed the crystals to be isostructural with those of 5Clura and 5Brura in the monoclinic space group $P2_1/m$ (Figure 1c). For this reason, the discussion of the crystal structure of 5Cl5Brura follows the above description. As with the two previous structures, in 5Cl5Brura the second carbonyl oxygen O2 is involved in an intermolecular contact [3.353 (3) Å] with the carbon atom C6 of adjacent noncentrosymmetric molecules. There are no indications of XBs, as the values of the shortest C5-Cl(Br)···O2 intermolecular contacts are 3.417 (2) and 3.316 (2) Å, respectively.

The asymmetric unit of 5Br1Mura, 4, comprises a molecule of the aminooxo tautomer in the monoclinic space group $P2_1/c$. Consistent with the earlier study, MBURAC [22], in the crystal centrosymmetric dimers via N3-H3···O2 hydrogen bonds are connected by the short C6-H6···O1 interaction [3.127 (3) Å] to form subunits of centrosymmetric $R_6^6(28)$ rings [34,35] (Table 2). These subunits are further stabilized by Br···Br interactions [d = 3.358 (2) Å] between two inversion-symmetric bromine atoms. Adjacent subunits then aggregate to form a layered structure (Figure 1d). No relevant intermolecular HBs or XBs involving the bromine atom of 5Br1Mura were observed.

Table 2. Hydrogen-bond geometries for compounds 1–4.

Compound	*D*-H···*A*	*D*-H (Å)	H···*A* (Å)	*D*···*A* (Å)	*D*-H···*A* (°)
1, 5Clura	N3-H3···O1^{i}	0.92	1.90	2.813 (2)	172
2, 5Brura	N3-H3···O1^{i}	0.87	1.95	2.819 (2)	175
3, 5Cl5Brura	N3-H3···O1^{i}	0.82	2.00	2.816 (2)	175
4, 5Br1Mura	N3-H3···O2^{ii}	0.80	2.04	2.839 (3)	176

Symmetry codes: (i) $-x, -y + 2, -z$; (ii) $-x + 1, -y, -z$.

3.2. Structural Analysis of 6-Halouracils (5–7)

The X-ray structural analysis of 6Clura, 6Iura, and 5Cl6Mura (5, 6, and 7 respectively) showed that the crystals are isostructural in the monoclinic space group $P2_1/c$. Consequently, the following discussion of their molecular disposition in the crystal will be the same.

Centrosymmetric dimers are hydrogen bonded by $R_2^2(8)$ motif involving the N3 donor and the O2 acceptor (Figure 2). These dimers are then connected via stronger N1-H1···O2 hydrogen bonds to adjacent dimers (the angle between these dimers is ca. 114°) (Table 3). All compounds display XBs in which the carbonyl oxygen atom O1, not involved in conventional HB interactions, acts as the XB acceptor. The structure of 5 has an almost linear C-Cl···O (3.04 Å, 166°) unit, whereas two shorter C-I···O and C-Cl···O (3.06 Å, 169° and 3.01 Å, 169°, respectively) units are found in 6 and 7, respectively. The XB ratios R_{XB} vary between 0.87 and 0.92, indicating weak to moderate interaction strength. No relevant intermolecular N-H···Cl(I) HBs are present in the structures.

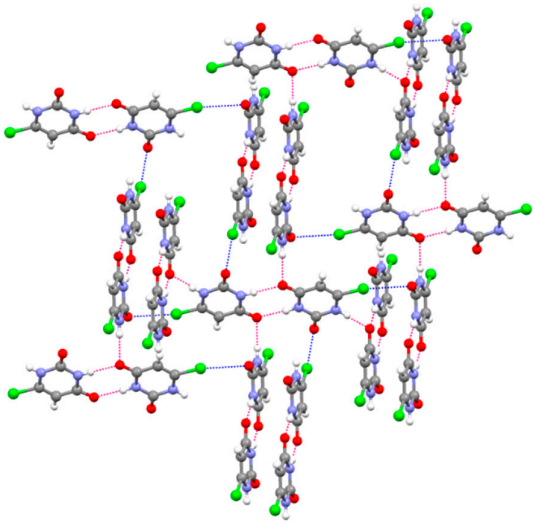

(**a**)

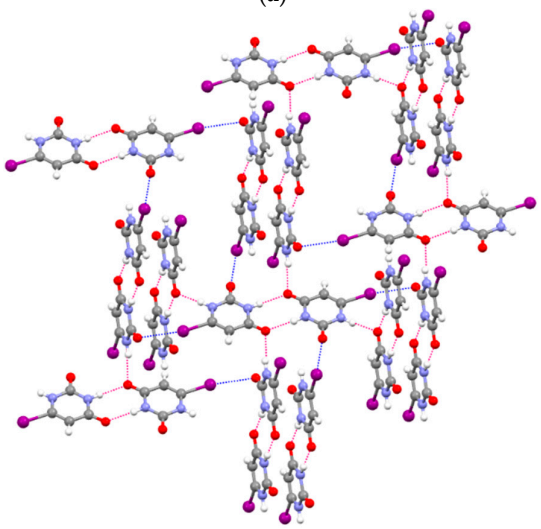

(**b**)

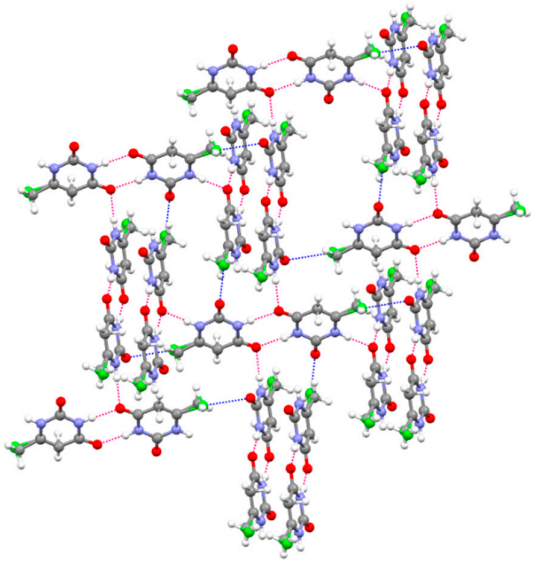

(**c**)

Figure 2. Hydrogen bonding and halogen bonding in the crystal packing of 6-halouracils. (**a**) 6Clura. (**b**) 6Iura. (**c**) 6Cl6Mura. Hydrogen bonds are shown as red dotted lines. Halogen bonds are shown as blue dotted lines.

Table 3. Hydrogen-bond geometries for compounds 5–7.

Compound	*D*-H···*A*	*D*-H (Å)	H···*A* (Å)	*D*···*A* (Å)	*D*-H···*A* (°)
5, 6Clura	N1-H1···O2^{i}	0.87	1.96	2.818 (3)	171
	N3-H3···O2^{ii}	0.88	1.96	2.841 (3)	178
6, 6Iura	N1-H1···O2^{i}	0.87	1.99	2.852 (4)	169
	N3-H3···O2^{ii}	0.87	2.01	2.873 (4)	175
7, 6Cl6Mura	N1-H1···O2^{i}	0.92	1.91	2.829 (2)	175
	N3-H3···O2^{ii}	0.91	1.94	2.843 (3)	176

Symmetry codes: (i) x, $-y + 1/2$, $z-1/2$; (ii) $-x$, $-y + 1$, $-z + 2$.

Regarding the effect of the crystal environment, characterized by XBs and N-H···O HBs of different strength, some general features emerge by comparing the geometry of the planar fragments O2=C4-C5-C6(-X)-N1 and O1=C2-N1, involved in both intermolecular interactions, with the geometry of the corresponding fragments obtained from a statistical survey of pyrimidine nucleobases in the Cambridge Structural Database [36] (Table 4). These features can be summarized as follows: (i) the C4-O2 carbonyl bond distances are longer by up to 0.016 (3) Å; (ii) the C4-C5 and C5-C6 bond distances are apparently equal within experimental error; (iii) the X-C6 bond distances are shorter by 0.021–0.029 (3) Å; (iv) C2-N1 and C6-N1 bond distances are shorter by 0.005–0.013 (4) Å and 0.013–0.021 (3) Å, respectively; (v) the C2-O1 carbonyl bond distances are longer by up to 0.008 (3) Å; (vi) the internal C5-C4-N3 bond angles are larger by 1.0–1.6 (3)°.

Table 4. Selected geometrical parameters (Å,°) for compounds 5–7.

Parameter	5, 6Clura	6, 6Iura	7, 6Cl6Mura	
Cl-C6	1.709 (3)	---	---	1.738 (6)[1]
I1-C6	---	2.076 (3)	---	2.097 (6)[2]
Cl-C6	---	---	1.715 (4)	1.738 (6)[1]
C5-C6	1.340 (4)	1.338 (4)	1.334 (3)	1.337 (1)[3]
C4-C5	1.428 (4)	1.431 (4)	1.425 (3)	1.431 (1)[3]
C4-O2	1.248 (3)	1.236 (4)	1.244 (3)	1.232 (1)[3]
C2-N1	1.376 (4)	1.373 (4)	1.368 (3)	1.381 (1)[3]
C6-N1	1.356 (3)	1.354 (4)	1.362 (3)	1.375 (1)[3]
C2-O1	1.227 (3)	1.224 (4)	1.218 (3)	1.219 (1)[3]
C5-C4-N3	116.2 (3)	115.6 (3)	116.1 (2)	114.6 (1)[3]

[1]QECNOB [37]. [2]From [38]. [3]From [36].

Therefore, the observed structural changes, though to the limits of statistical relevance, taken together can suggest, in terms of Valence Bond theory, some degree of delocalization of π-electron density through a slight increase in the contribution of polar canonical form (I)–(III) (Figure 3). On one hand forms (I) and (III) are better halogen donors and halogen acceptors at O1. On the other hand, forms (I)–(III), as N-H-O hydrogen bonds become progressively stronger as a partial charge is accumulated on the nitrogen and oxygen atoms [39,40], are better hydrogen donors at N1 and hydrogen acceptor at O2 than the neutral canonical form.

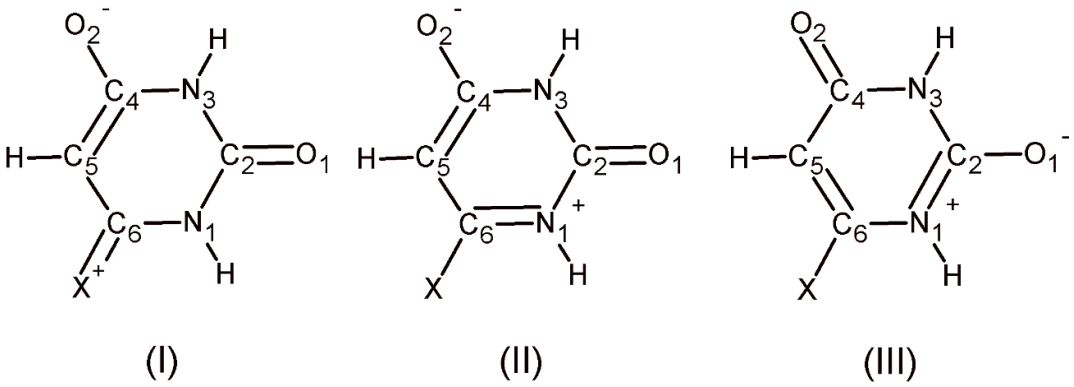

Figure 3. Possible polar canonical forms for compounds 5–7.

3.3. Hirshfeld Surface Analysis

Hirshfeld surface analysis was performed to give insights regarding the important intermolecular interactions in the crystals. 3D Hirshfeld surfaces were mapped over d_{norm}, the ratio encompassing the distances of any surface point to the nearest interior (d_i) and exterior (d_e) atom and the vdW radii of the atom, using a high (standard) surface resolution. These surfaces enable the visualization of intermolecular contacts over the surface by different colors and color intensity. Strong, neutral, and weak interactions involved in the stabilization of crystal structure were visualized as red, white and blue colors, respectively [41]. Two-dimensional fingerprint plots over the Hirshfeld surfaces were used to highlight the nature of the intermolecular interactions for crystal packing, and the different colors on the fingerprint plot represent the frequency of occurrence of the interactions, increasing from blue to green to red. For the generation of fingerprint plots, the bond lengths involving hydrogen atoms were normalized to standard neutron values (O-H = 0.983 Å, N-H = 1.009 Å, C-H = 1.083 Å).

3.3.1. Hirshfeld Surface Analysis of 5-Halouracils (1–4)

The 3D d_{norm} Hirshfeld surface plots of the four 5-halouracils are shown in Figure 4. The large and deep red spots on the surfaces indicate the areas where close-contact interactions due to strong hydrogen bonds take place.

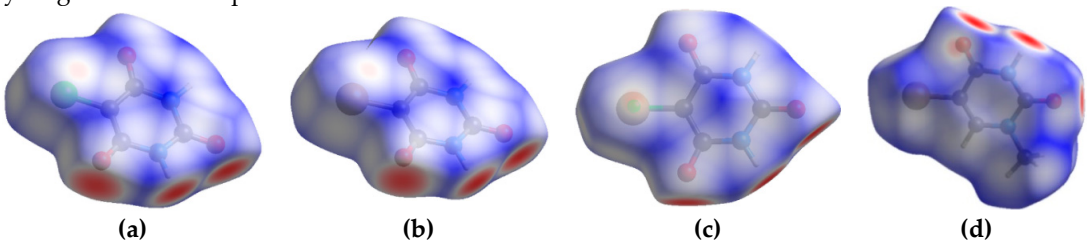

Figure 4. Hirshfeld surfaces mapped on d_{norm}. (**a**) 5Clura; color scale: −0.619 (red) –0.922 a.u. (blue). (**b**) 5Brura; color scale: −0.616 (red) –0.950 a.u. (blue). (**c**) 5Cl5Brura; color scale: –0.619 (red) –0.973 a.u. (blue). (**d**) 5Br1Mura; color scale: −0.601 (red) –0.992 a.u. (blue).

As the crystallographic investigation of the 5Clura, 5Brura, and 5Cl5Brura (1, 2 and 3, respectively) showed the crystals to be isostructural in the monoclinic space group $P2_1/m$, the overall two-dimensional fingerprint plot and the plots illustrating close contacts and their proportional contributions will be shown only for 5Clura (Figure 5). For the sake of comparison, contributions of the intermolecular contacts for 5Brura and 5Cl5Brura are summarized in Table 5. The fingerprint plots of all structures show similar features about intermolecular interactions. Long spikes, characteristics for strong hydrogen bonds, for O···H pairwise interaction were found to have similar

contributions and are the most significant over the total Hirshfeld surfaces (23.6–23.9%). Other important contacts, such as O···O (10.4–12.4%), O···C/C···O (7.5–11.5%), Cl(Br)···O/O···Cl(Br) (11.3–11.4%) and Cl(Br)···H/H···Cl(Br) (9.3–11.3%) also supplement the overall crystal packing.

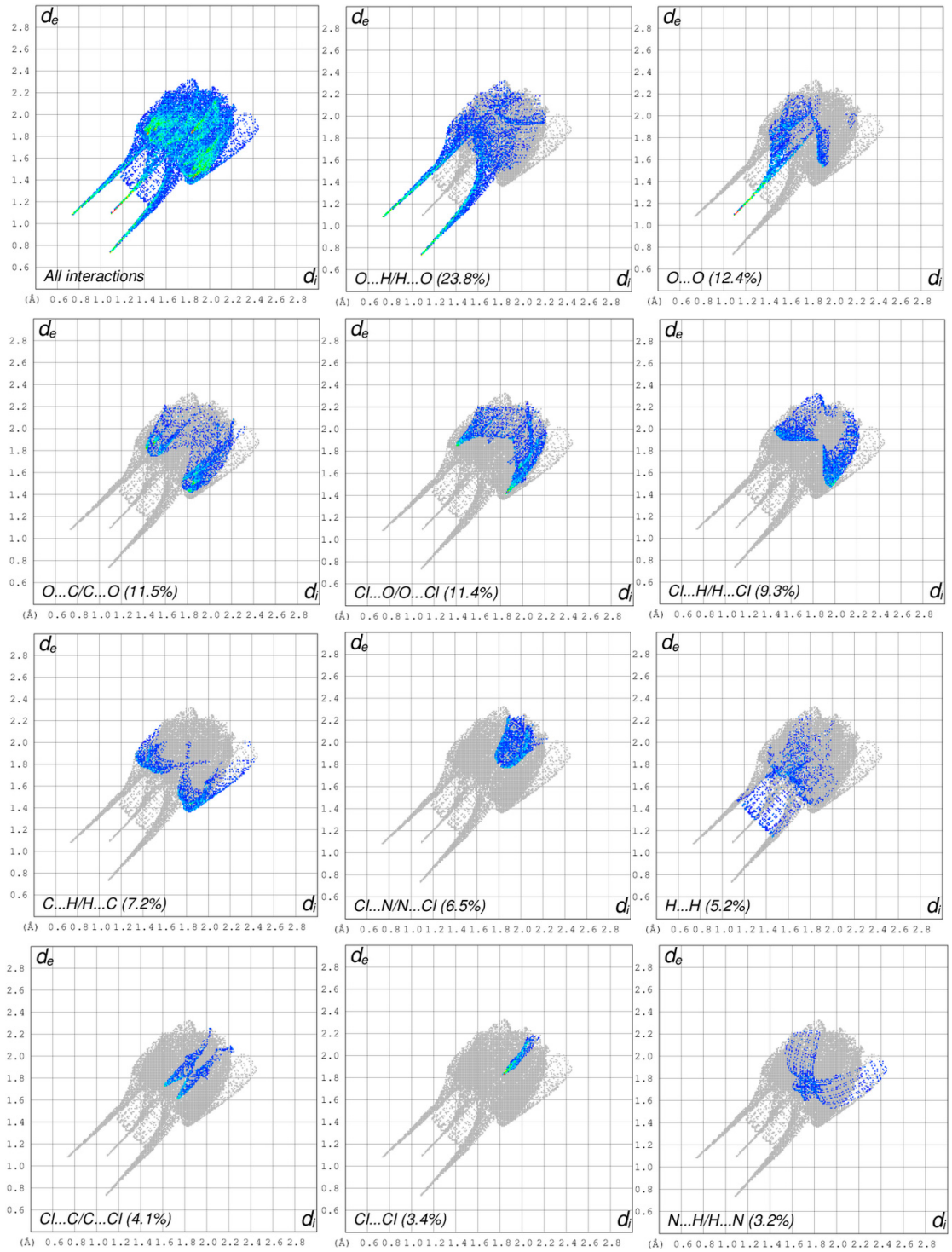

Figure 5. Decomposed two-dimensional fingerprint plots for 5Clura. Various close contacts and their proportional contributions are reported. Other (not shown) intermolecular contacts contribute approximately 2% to the Hirshfeld surface mapping.

Table 5. Contributions of the intermolecular contacts for compounds 2 and 3.

Contact (%)	2, 5Brura	3, 5Cl5Brura
O···H/H···O	23.6	23.9
O···O	10.4	12.1
O···C/C···O	8.6	7.5
Cl···O/O···Cl	---	5.7
Br···O/O···Br	11.3	5.8
Cl···H/H···Cl	---	1.5
Br···H/H···Br	11.3	9.8
C···H/H···C	8.5	9.8
Cl···N/N···Cl	---	4.3
Br···N/N···Br	5.4	1.1
H···H	7.4	4.9
Cl···C/C···Cl	---	3.4
Br···C/C···Br	3.9	0.5
Cl···Cl	---	0.7
Br···Br	3.9	0.1
N···H/H···N	0.9	1.2

The overall two-dimensional fingerprint plot and the plots illustrating close contacts and their proportional contributions in 5Br1Mura are shown in Figure 6. The increased amount of combined O···H/H···O (36.6%), Br···H/H···Br (17.2%), and H···H (14.0%) interactions compared to the previous structures is in accordance with the replacement of a hydrogen atom with a methyl group. As with the previous structures, the dominant interactions between H and O atoms (long spikes in the fingerprint plot) correspond to the hydrogen bonds discussed above. Other contacts, such as C···H/H···C (7.6%), Br···C/C···Br (4.3%), O···C/C···O (3.8%), Br···N/N···Br (3.6%), Br···Br (2.9%), N···H/H···N (2.8%), Br···O/O···Br (2.7%), and C···C (2.6%) also make significant contributions to the Hirshfeld surface.

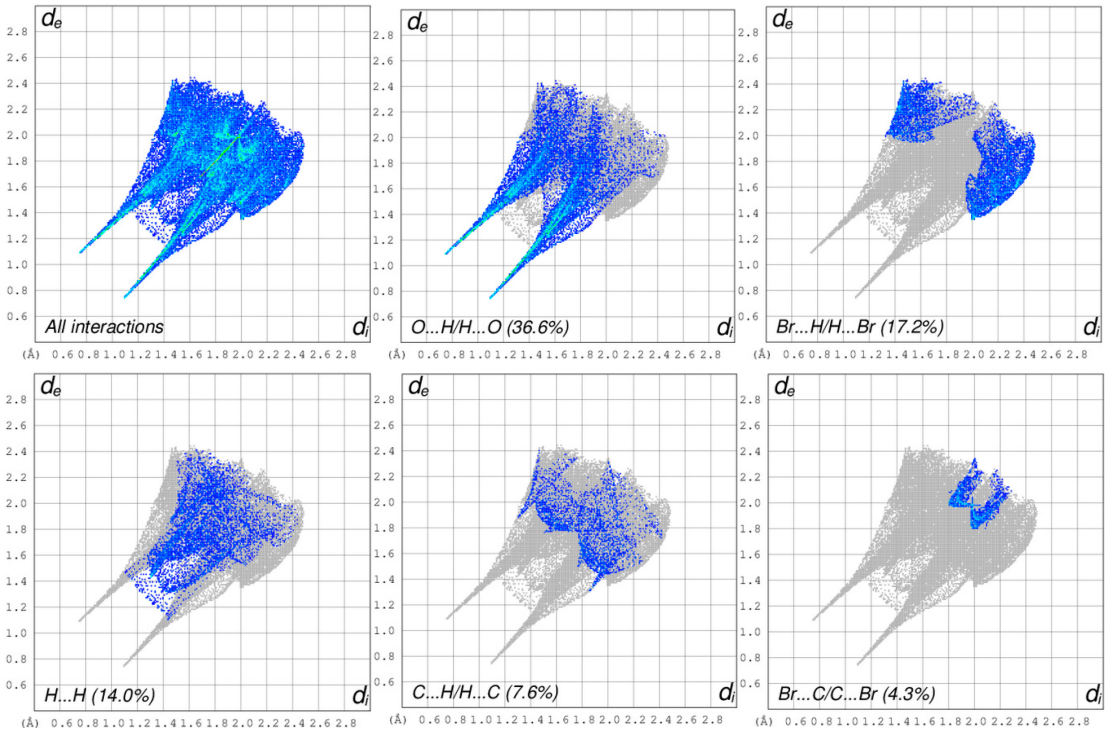

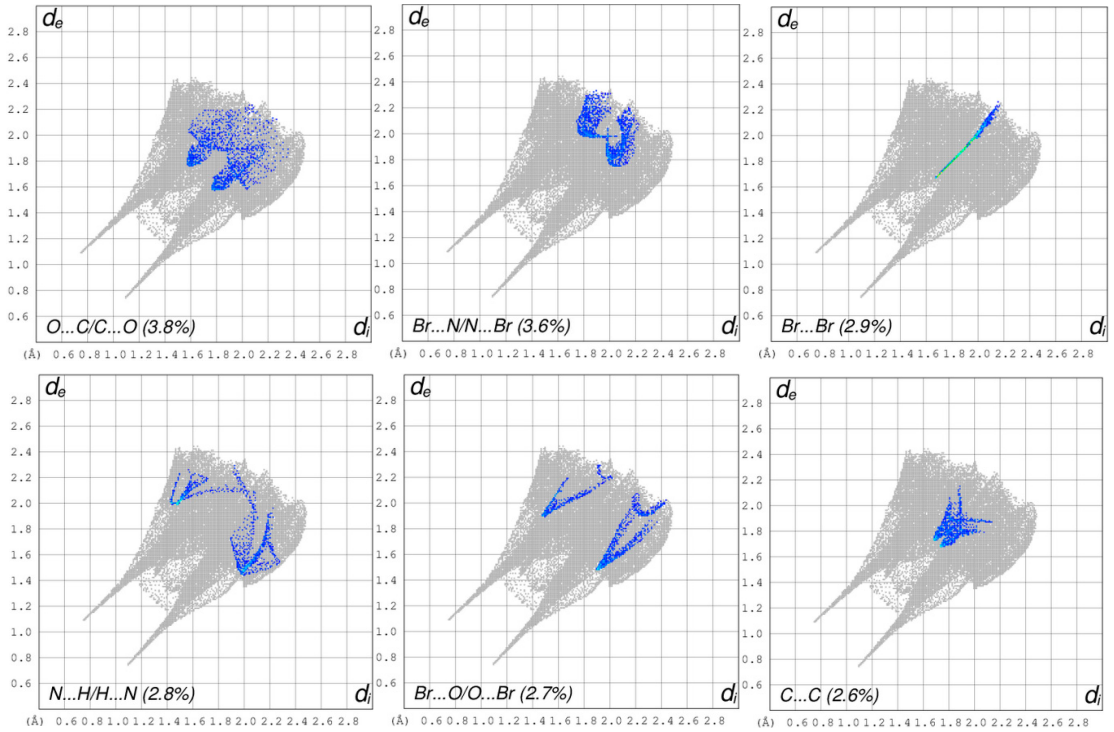

Figure 6. Decomposed two-dimensional fingerprint plots for 5Br1Mura. Various close contacts and their proportional contributions are reported. Other (not shown) intermolecular contacts contribute approximately 1% to the Hirshfeld surface mapping.

3.3.2. Hirshfeld Surface Analysis of 6-Halouracils (5–7)

Hirshfeld surfaces of the three 6-halouracils were mapped over the normalized distance, d_{norm}, and are shown in Figure 7. The 3D d_{norm} surfaces infer both the hydrogen and halogen bond previously noted, as red spots due to the distance between the interaction sites are below the vdW interaction. However, the intensity of the red spot varies from high, due to strong hydrogen bond, to faint, due to the close contact by C=O···Cl(I).

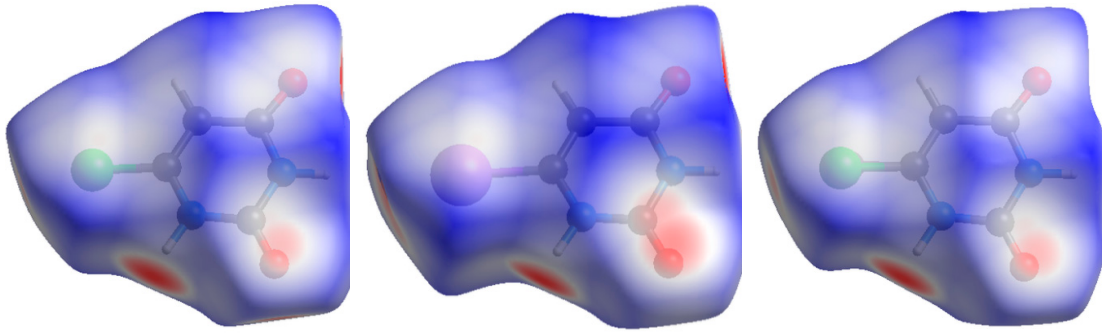

(**a**) (**b**) (**c**)

Figure 7. Hirshfeld surfaces mapped on d_{norm}. (**a**) 6Clura; color scale: –0.583 (red) –1.024 a.u. (blue). (**b**) 6Iura; color scale: –0.614 (red) –1.091 a.u. (blue). (**c**) 6Cl6Mura; color scale: –0.609 (red) –1.115 a.u. (blue).

As already mentioned, 6Clura, 6Iura, and 5Cl6Mura (5, 6, and 7 respectively) are isostructural in the monoclinic space group $P2_1/c$. Consequently, the overall two-dimensional fingerprint plot and the plots illustrating close contacts and their proportional contributions will be shown only for 6Iura, in which the R_{XB} shows the smallest value (0.87) (Figure 8). For the sake of comparison, contributions

of the intermolecular contacts for 6Clura and 6Cl6Mura are summarized in Table 6. The fingerprint plots of 6-halouracils show similar features about intermolecular interactions. It could be observed that the O···H pairwise contact displays major contribution in crystal packing cohesion, with 36.8–37.6% of total surface area. The I(Cl)···C and I(Cl)···O pairwise contacts, appearing as two blunt spikes, with second and third major contribution comprise 8.6–11.0% and 8.3–10.8% of total surface area, respectively. Apart from those, H···H, I(Cl)···H, C···H and O···C pairwise contacts also show important contributions for the molecular aggregation from 9.8% to 3.1% of total surface area in the fingerprint plot.

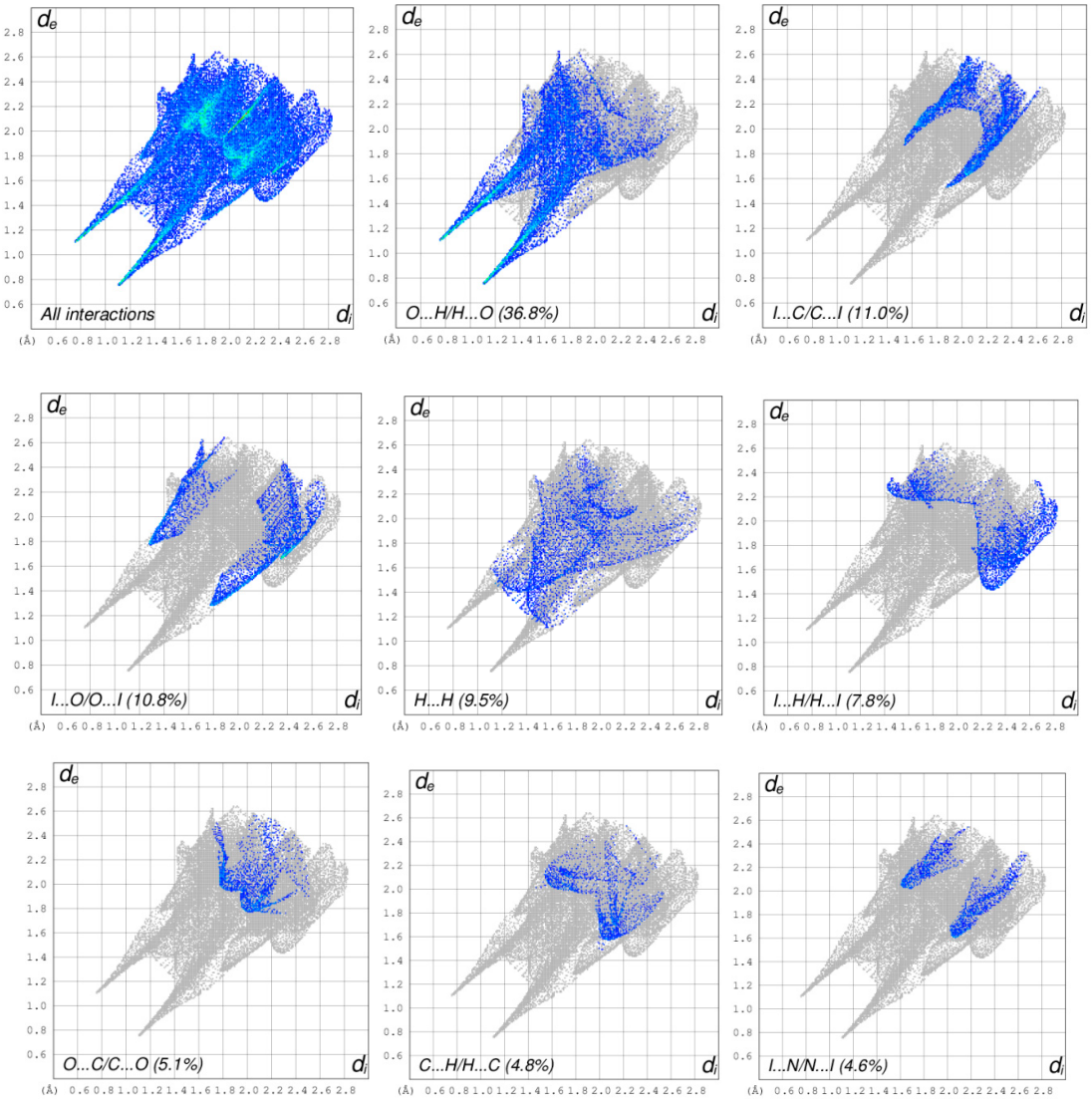

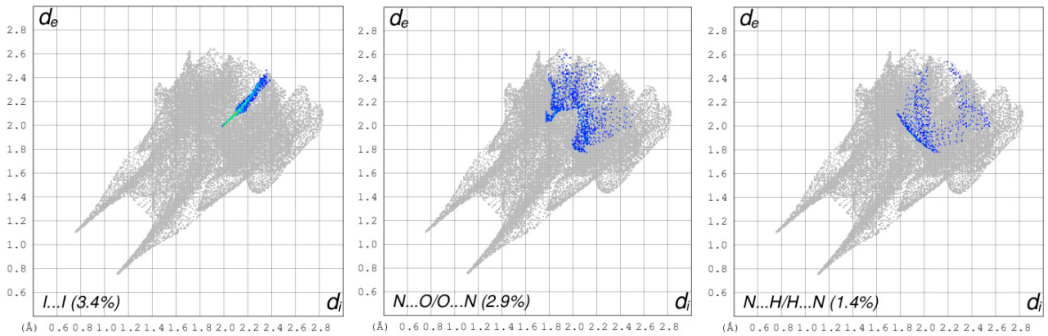

Figure 8. Decomposed two-dimensional fingerprint plots for 6Iura. Various close contacts and their proportional contributions are reported. Other (not shown) intermolecular contacts contribute less than 2% to the Hirshfeld surface mapping.

Table 6. Contributions of the intermolecular contacts for compounds 5 and 7.

Contact (%)	5, 6Clura	7, 6Cl6Mura
O···H/H···O	37.4	36.8
Cl···C/C···Cl	10.8	8.6
Cl···O/O···Cl	9.4	8.3
H···H	9.8	9.6
Cl···H/H···Cl	6.9	3.1
O···C/C···O	5.8	7.9
C···H/H···C	4.9	8.8
Cl···N/N···Cl	3.7	3.5
Cl···Cl	3.3	0.9
N···O/O···N	4.3	4.3
N···H/H···N	1.5	1.5

4. Conclusions

The purpose of this study was to ascertain the existence and the preferred donor and acceptor sites of halogen bonds (C-O···X) in the presence of hydrogen bonds in pure pyrimidine nucleobases halosubstituted at the 5- and 6-position. Seven crystal structures consisting of either 5Xuras (1–4) or 6Xuras (5–7) were determined by XRD.

The following conclusions summarize the findings of this work:

1) In pure 5-halo and 6-halouracils, no halogen mediated HBs were observed. In the crystals of 5-halouracils, capable of forming XBs, the dominant role of conventional and unconventional hydrogen bonds prevents the formation of halogen bonds between the uracil units.

2) Halogen bonding is present in 6-halouracils, and the preferred acceptor site for XB interaction is the urea carbonyl oxygen O1, which does not take part in conventional HBs.

3) The halogen bonds in 6-halouracils are all rather weak, as supported by the Hirshfeld surface analysis. The strongest interaction was found in the structure of **6**, 6Iura, which displayed the largest (13%) reduction of the sum of vdW radii for the contact atoms. Despite this, halogen bonding plays a role in determining the crystal packing of all three compounds, acting alongside conventional hydrogen bonds, which are the primary structure-directing interactions.

The work presented here is purely observational and could be substantiated with theoretical calculations which will be performed in the future.

Supplementary Materials: The following are available online at www.mdpi.com/xxx/s1. Figures S1–S7 showing the Ortep diagrams for the seven compounds studied.

Funding: This research received no external funding.

Conflicts of Interest: The author declares no conflict of interest.

References

1. Fourmiguè, M.; Batail, P. Activation of Hydrogen- and Halogen-Bonding interactions in tetrathiafulvalene-based crystalline molecular conductors. *Chem. Rev.* **2004**, *104*, 5379–5418.
2. Parker, A.J.; Stewart, J.; Donald, K.J.; Parish, C.A. Halogen bonding in DNA base pairs. *J. Am. Chem. Soc.* **2012**, *134*, 5165–5172.
3. Voth, A.R.; Hays, F.A.; Ho, P.S. Directing macromolecular conformation through halogen bonds. *Proc. Natl Acad. Sci.* **2007**, *104*, 6188–6193.
4. Cavallo, G.; Metrangolo, P.; Milani, R.; Pilati, T.; Primagi, A.; Resnati, G.; Terraneo, G. The halogen bond. *Chem. Rev.* **2016**, *116*, 2478–2601.
5. Auffinger, P.; Hays, F.A.; Westhof, E.; Ho, P.S. Halogen bonds in biological molecules. *Proc. Natl. Acad. Sci.* **2004**, *101*, 16789–16794.
6. Peterson, M.L.; Hickey, M.B.; Zaworotko, M.J.; Almarsson, Ö. Expanding the scope of crystal form evaluation in pharmaceutical science. *J. Pharm. Pharm. Sci.* **2006**, *9*, 317–326.
7. Groom, C.R.; Allen, F. The cambridge structural database in retrospect and prospect. *Angew. Chem. Int. Ed.* **2014**, *53*, 662–671.
8. Portalone, G.; Moilanen, J.; Tuononen, H.M.; Rissanen, K. Role of weak hydrogen bonds and halogen bonds in 5-Halo-1,3-dimethyluracils and their cocrystals—A combined experimental and computational study. *Cryst. Growth Des.* **2016**, *16*, 2631–2639.
9. Valkonen, A.; Chukhlieb, M.; Moilanen, J.; Tuononen, H.M.; Rissanen, K. Halogen and hydrogen bonded complexes of 5-Iodouracil. *Cryst. Growth Des.* **2013**, *13*, 4769–4775.
10. Gerhardt, V.; Egert, E. Cocrystals of 6-chlorouracil and 6-chloro-3-methyl-uracil: exploring their hydrogen-bond-based synthon motifs with several triazine and pyrimidine derivatives. *Acta Cryst. B* **2015**, *71*, 209–220.
11. Portalone, G.; Rissanen, K. Multifacial recognition in binary and ternary cocrystals from 5-halouracil and aminoazine derivatives. *Cryst. Growth Des.* **2018**, *18*, 5904–5918.
12. Portalone, G.; Colapietro, M.; Ramondo, F.; Bencivenni, L.; Pieretti, A. The effect of the hydrogen bonding on the structures of uracil and some methyl derivatives studied by experiment and theory. *Acta Chem. Scand.* **1999**, *53*, 57–68.
13. Brunetti, B.; Piacente, V.; Portalone, G. Sublimation thermodynamics parameters for 5-fluorouracil and its 1-methyl and 1,3-dimethyl derivatives from vapor pressures measurements. *J. Chem. Eng. Data* **2002**, *47*, 17–19.
14. Portalone, G.; Colapietro, M. First example of cocrystal of polymorphic maleic hydrazide. *J. Chem. Cryst.* **2004**, *34*, 609–612.
15. Portalone, G.; Colapietro, M.; Asymmetric base pairing in the complex 5-Fluorocytosinium chloride/5-Fluorocytosine monohydrate. *J. Chem. Cryst.* **2007**, *37*, 141–145.
16. Portalone, G.; Colapietro, M. Unusual syn conformation of 5-formyluracil stabilized by supramolecular interactions. *Acta Cryst. C* **2007**, *63*, o650–o654.
17. Portalone, G. Redetermination of 5-iodouracil. *Acta Cryst. E* **2008**, *64*, o365.
18. Portalone, G. Supramolecular association in proton-transfer adducts containing benzamidinium cations. I. Four molecular salts with uracil derivatives. *Acta Cryst. C* **2010**, *66*, o295–o301.
19. Habgood, M.; Price, S.L.; Portalone, G.; Irrera, S.J. Testing a variety of electronic-structure-based methods for the relative energies of 5-formyluracil crystals. *Chem. Theor. Comp.* **2011**, *7*, 2685–2688.
20. Irrera, S.; Roldan, A.; Portalone, G.; de Leeuw, N.H. The role of hydrogen bonding and proton transfer in the formation of uracil networks on the gold (100) surface: a density functional theory approach. *J. Phys. Chem. C* **2013**, *117*, 3949–3957.
21. Brunetti, B.; Irrera, S.; Portalone, G. Sublimation Enthalpies of 5-Haloderivatives of 1,3-Dimethyluracil. *J. Chem. Eng. Data* **2015**, *60*, 74–81.
22. Mizuno, H.; Morita, K.; Fujiwara, T.; Tomita, K.I. The crystal and molecular structure of 1-methyl-5-bromouracil and some structural considerations on the mutation mechanism. *Chem. Lett.* **1972**, *10*, 965–968.
23. Bader, R.F.W. A quantum theory of molecular structure and its applications. *Chem. Rev.* **1991**, *91*, 893–928.

24. Adonin, S.A.; Gorokh, I.D.; Novikov, A.S.; Samsonenko, D.G.; Yushina, Y.V.; Sokolov, M.N.; Fedin, V.P. Halobismuthates with halopyridinium cations: Appearance or non-appearance of unusual colouring. *Cryst. Eng. Comm.* **2018**, *20*, 7766–7772.
25. Gorokh, I.D.; Adonin, S.A.; Novikov, A.S.; Usoltsev, A.N.; Plyusnin, P.E.; Korolkov, I.V.; Sokolov, M.N.; Fedin, V.P. Halobismuthates with 3-iodopyridinium cations: Halogen bonding-assisted crystal packing. *Polyhedron* **2019**, *166*, 137–140.
26. *CrysAlis PRO*, Version 1.171.35.19. Agilent Technologies Ltd: Yarnton, Oxfordshire, Yarnton, England, 2014.
27. Burla, M.C.; Caliandro, R.; Camalli, M.; Carrozzini, B.; Cascarano, G.L.; De Caro, L.; Giacovazzo, C.; Polidori, G.; Spagna, R. SIR2004: An improved tool for crystal structure determination and refinement. *J. Appl. Cryst.* **2005**, *32*, 115–119.
28. Sheldrick, G.M. Crystal structure refinement with SHELXL. *Acta Cryst. C* **2015**, *71*, 3–8.
29. Farrugia, L.J. WingX and ORTEP for Windows: An update. *J. Appl. Cryst.* **2012**, *45*, 849–854.
30. Macrae, C.F.; Bruno, I.J.; Chisholm, J.A.; Edgington, P.R.; McCabe, P.; Pidcock, E.; Rodriguez-Monge, L.; Taylor, R.; van de Streek, J.; Wood, P.A. New features for the visualization and investigation of crystal structures. *J. Appl. Crystallogr.* **2008**, *41*, 466–470.
31. *CrystalExplorer,* Version 3.1; University of Western Australia: Crawley, AU, Australia, 2005–2013.
32. Sternglanz, H.; Bugg, C.E. Relationship between the mutagenic and base stacking properties of halogenated uracil derivatives. The crystal structures of 5-chloro- and 5-bromouracil. *Biochim. Biophys. Acta* **1975**, *378*, 1–11.
33. Barnett, S.A.; Hulme, A.T.; Issa, N.; Lewis, T.C.; Price, L.S.; Tocher, D.A.; Price, S.L. The observed and energetically feasible crystal structures of 5-substituted uracils. *New J. Chem.* **2008**, *32*, 1761–1775.
34. Etter, M.C.; MacDonald, J.C.; Bernstein, J. Graph-Set analysis of hydrogen-bond patterns in organic crystals. *Acta Cryst. B* **1990**, *46*, 256–262.
35. Bernstein, J., Davis, R.E., Shimoni, L.; Chang, N.L. Patterns in hydrogen bonding: functionality and graph set analysis in crystals. *Angew. Chem. Int. Ed. Engl.* **1995**, *34*, 1555–1573.
36. Clowney, L.; Jain, S.C.; Srinivasan, A.R.; Westbrook, J.; Olson, W.K.; Berman, H.M. Geometric parameters in nucleic acids: Nitrogenous bases. *J. Am. Chem. Soc.* **1996**, *118*, 509–518.
37. Schmidt, A.; Kindermann, M.K.; Vainiotalo, P.; Nieger, M. Charge-Separated modified nucleobases. on π-interactions and hydrogen bonding of self-complementary cationic and betainic uracils. *J. Org. Chem.* **1999**, *64*, 9488–9506.
38. Mondal, S.; Manna, D.; Mugesh, G. Selenium-Mediated dehalogenation of halogenated nucleosides and its relevance to the DNA repair pathway. *Angew. Chem. Int. Ed. Engl.* **2015**, *54*, 9298–9302.
39. Taylor R.; Olga Kennard, O. Hydrogen-Bond geometry in organic crystals. *Acc. Chem. Res*. **1984**, *17*, 320–326.
40. Steiner, T. The hydrogen bond in the solid state. *Angew. Chem. Int. Ed. Engl.* **2002**, *41*, 48–76.
41. Spackman, M.A.; Jayatilaka, D. Hirshfeld surface analysis. *Cryst. Eng. Comm.* **2009**, *11*, 19–32.